



Full Length Article

A novel method for widely tunable semiconductor lasers: Temperature-induced gain spectrum shift between adjacent grating reflection peaks

Yinli Zhou^{*}, Xing Zhang, Jianwei Zhang, Yongqiang Ning, Yugang Zeng, Lijun Wang

State Key Laboratory of Luminescence and Applications, Changchun Institute of Optics, Fine Mechanics and Physics, Chinese Academy of Sciences, Changchun, 130033, China



ARTICLE INFO

Keywords:

Widely tunable semiconductor lasers
Temperature-induced gain spectrum shift
Adjacent grating reflection peaks
High-order surface gratings

ABSTRACT

We report a slotted high-order surface grating semiconductor laser without a multi-section design. A wide tuning range of 20 nm with side mode suppression ratios (SMSRs) larger than 30 dB is realized by controlling the temperature and the injection current. With a temperature variation of 30 °C, the wavelength tuning range is larger than 10 nm, in contrast to ~3 nm for thermo-optic tuning range in other grating-based lasers. By analyzing the gain and the reflection spectrum of the device, we attribute this wide tuning range to the movement of the temperature-induced gain spectrum between the two adjacent Bragg reflection peaks of high-order surface gratings. This is a new method to realize the wide wavelength tuning range.

1. Introduction

Widely tunable semiconductor lasers are well suited for numerous applications in communications and spectroscopy [1–4]. A variety of monolithic integrated tunable semiconductor lasers have been developed, such as distributed feedback (DFB) lasers, distributed Bragg reflector (DBR) lasers and Fabry-Pérot (F-P) lasers with surface etched slots. Based on thermal-optical effects, a single DFB laser can only tune about 4 nm [5]. A DBR laser with one grating section can achieve a tunable range of 20 nm by changing the carrier density and temperature in the grating region [6]. Based on sampling grating structures and Vernier effect, multi-section DBR lasers can realize a tuning range over 50 nm [7–10]. Coupled cavity lasers can achieve a tuning range of 50 nm by combining temperature-assisted gain spectrum shift with vernier effect [11]. F-P lasers with high-order surface gratings can be fabricated without high resolution lithography and secondary epitaxy, which greatly reduces manufacturing difficulty [12–18]. A tuning range over 30 nm is achieved based on a four-sections slotted surface grating structure fabricated by standard resolution lithography [12]. And a tuning range of 55 nm with SMSR >30 dB is reported for a semiconductor laser with six sections based on etched slots [13].

Most of the wavelength tuning principles mentioned above are based on carrier-induced refractive index variation and vernier effect of the

gratings. In order to use the vernier effect, multiple grating sections and therefore multiple electrodes are required. A slotted high-order surface gratings semiconductor laser without multiple sections and electrodes is demonstrated in this letter. Depends on the common tuning of current and temperature, the device realized a wide tuning range of 20 nm. Preliminary analysis attributed the mechanism of this wide tuning to the temperature-induced gain spectrum movement between two adjacent Bragg reflection peaks of the gratings. It is, to our knowledge, a new method to realize the wide wavelength tuning range, which is different from the abovementioned mechanism. The basic structure of the article is as follows: First, the device structure and the design of the gratings is introduced. Then, the device performance is presented such as spectral characteristics, power-current characteristics, and wavelength tuning range. Finally, the mechanism of wide tuning is analyzed theoretically.

2. Device structure and grating design

A schematic drawing of the epitaxial layer structure and the implementation of the grating and the ridge waveguide is depicted in Fig. 1. The epitaxial structure of the device contains a symmetrical waveguide layer with 1.2 μm, and a 10 nm InGaAs/GaAs quantum well with In content of 0.28 in the middle of the waveguide layer. The thickness of the cladding layers above and below the waveguide layer is 1.4 μm. The

^{*} Corresponding author.

E-mail address: zhouyinli@ciomp.ac.cn (Y. Zhou).

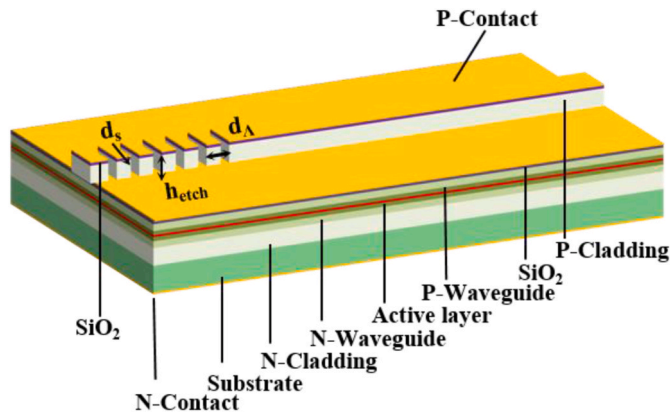


Fig. 1. The 3D device structure of the DBR laser.

GaAs cap layer is 100 nm. The devices have a total length of 3 mm and a ridge width of 4 μm. The grating parameters include grating period d_{Λ} , slot width d_s , etching depth h_{etch} , and the number of gratings N .

In order to obtain the best grating parameters, the finite element method (FEM) and two-dimensional scattering matrix method (SMM) were used. The refractive index difference caused by the surface etching slot structure makes the optical field at the grating section exhibit obvious Bragg feedback characteristics. The S parameter of a single grating varies with wavelength and can be obtained by parametric scanning. Then the reflectivity and loss curves of multiple pairs of gratings were calculated by the SMM method. The detailed analytical method and conclusions have been already fully described in previous research [19]. Through the method of controlling variables, the influences of the four grating parameters d_{Λ} , d_s , h_{etch} , and N on the reflectivity of the grating are studied respectively. As can be seen from Fig. 2(a), when the wavelength is set to 1064 nm and the grating number is set to 200, the reflectivity changes periodically with the grating period. The interval between two adjacent grating periods is 157 nm. At different etching depths, the change of reflectivity with the number of

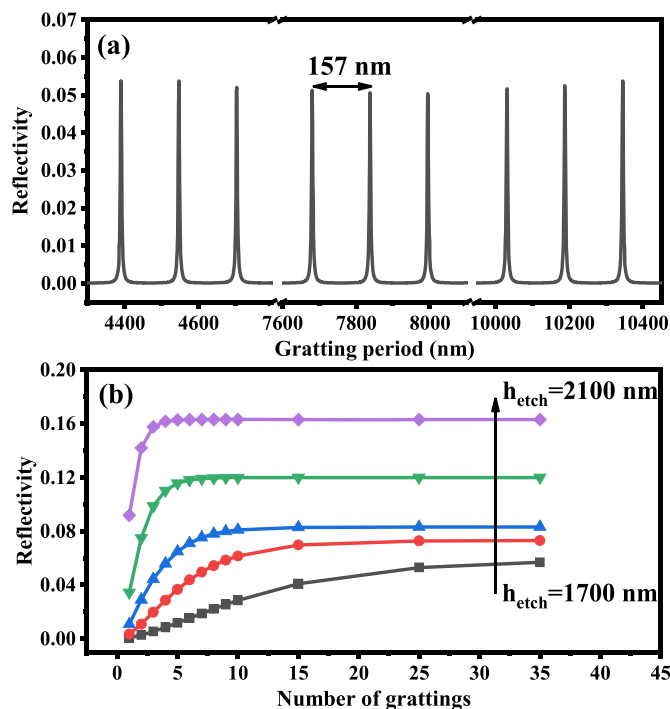


Fig. 2. Effect of (a) grating period and (b) number of gratings on the reflectivity at the wavelength of 1064 nm.

grating N is shown in Fig. 2(b). For deep slots, reflection saturates rapidly as the number of gratings increases due to relatively large scattering losses. When the slot depth is 1.7 μm, the reflection begins to saturate at N is 35. And the reflectivity increases as the etching depth of the grating increase.

Fig. 3 shows the effect of slot width d_s and etching depth h_{etch} on the reflectivity of the grating. As can be seen from Fig. 3(a), when d_s increase, the center wavelength appears blue-shifted, and the peak reflectivity decreases, and a full width at half maxima (FWHM) of the reflectivity is almost unchanged. Fig. 3(b) depicts that as h_{etch} increases, the peak reflectivity and the FWHM are both increasing, and the peak position is slightly blue-shifted.

Based on the above conclusions, the final grating parameters used are as follows: $d_{\Lambda} = 7681$ nm, $d_s = 1500$ nm, $h_{etch} = 1900$ nm, $N = 15$. The order of grating calculated by the Bragg formula is 49. The peak reflectivity of 8.3% near 1064 nm and a ~3 nm FWHM of reflectivity spectrum that is beneficial to realize single longitudinal mode lasing [20] have been achieved. The distance between two adjacent reflection peak positions is ~21 nm.

3. Experimental results and discussions

The epitaxial structure of the DBR lasers was grown by MOCVD on an GaAs substrate. The grating and ridged waveguide structures were fabricated by standard photolithography and dry etching processes. The SiO₂ electrical insulation layer is 300 nm and deposited by Plasma-Enhanced Chemical Vapor Deposition (PECVD). Metal electrodes were deposited on the top and back of the wafer by magnetron sputtering, respectively. After the alloying process, the wafer was cleaved into a single chip, which is flip chip bonded on aluminum nitride (AlN) carrier. A thermal-electric cooler (TEC) is used for temperature control, and the accuracy is 0.1 °C. A multi-mode fiber is used to collect the light emitted by the laser chip and transmit it into spectrometer for analysis. The resolution of the spectrometer is set to 0.02 nm.

Fig. 4(a) depicts the lasing spectrum with current at the temperature of 17 °C. The single longitudinal mode performance of the device is stable, and the highest SMSR reaches 43 dB. The peak wavelength redshift from 1058.3 nm to 1062 nm with current change from 100 mA to 700 mA. The lasing wavelength shows an obvious redshift as the

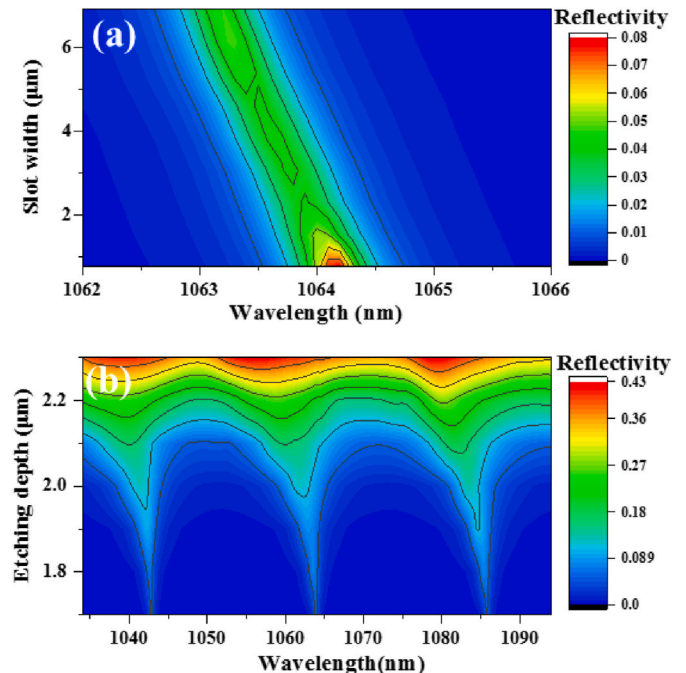


Fig. 3. Effect of (a) slot width and (b) etching depth on the reflectivity.

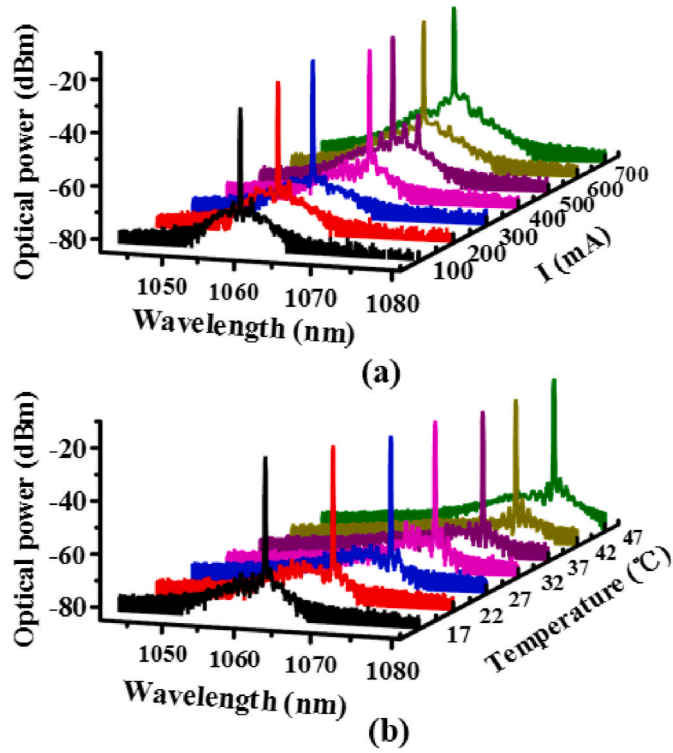


Fig. 4. (a) Spectrum with different currents under 17 °C. (b) Spectrum with different temperatures under 400 mA.

current changes from 300 mA to 400 mA and a slight blueshift as the current changes from 600 mA to 700 mA. This is primarily due to the effects of gain on wavelength tuning caused by carrier density change, which is consistent with the research conclusions of Ref [21]. Fig. 4(b) shows the lasing spectrum with temperature at the current of 400 mA. The peak wavelength redshift from 1061.7 nm to 1074.4 nm with temperature change from 17 °C to 47 °C.

Fig. 5(a) shows the spectrum of 20 different wavelengths measured from the laser, covering a range of 20 nm. The interval between the two adjacent wavelengths is 1 nm and the SMSR of each wavelength is over 30 dB. The variation of the SMSR with the lasing wavelength is depicted in Fig. 5(b). The current changed from 100 mA to 700 mA with a step of 100 mA and the temperature changed from 17 °C to 47 °C with a step of 1 °C. Points with SMSR below 20 dB are not drawn. The SMSR is mainly concentrated in 35 dB–45 dB. All of the emission wavelengths within the wavelength range can be accessed with the help of tuning injection current and temperature. Fig. 5(c) depicts the peak wavelength changes with temperature under different currents. At each current condition, a temperature change of 30 °C produces a wavelength tuning range greater than 10 nm. In contrast, other tunable lasers based on refractive index changes have a wavelength drift rate of only 0.1 nm/°C with temperature, and a wavelength tuning range of only around 3 nm with a temperature change of 30 °C [18,22]. The device in this paper only contains uniform high-order surface grating and does not use a multi-section design to form electrical isolation between the grating and the gain region. Therefore, the wide tuning range is not achieved through the vernier effect.

In order to investigate further the mechanism of the wide wavelength-tunable range of our device, the loss and gain spectrum with the temperature of the device at fixed carrier density was analyzed. The threshold condition of the semiconductor laser can be expressed by the formula:

$$\Gamma g_{\text{material}} = \alpha_i + \frac{1}{2L} \ln \frac{1}{R_f R_{\text{DBR}}} \quad (1)$$

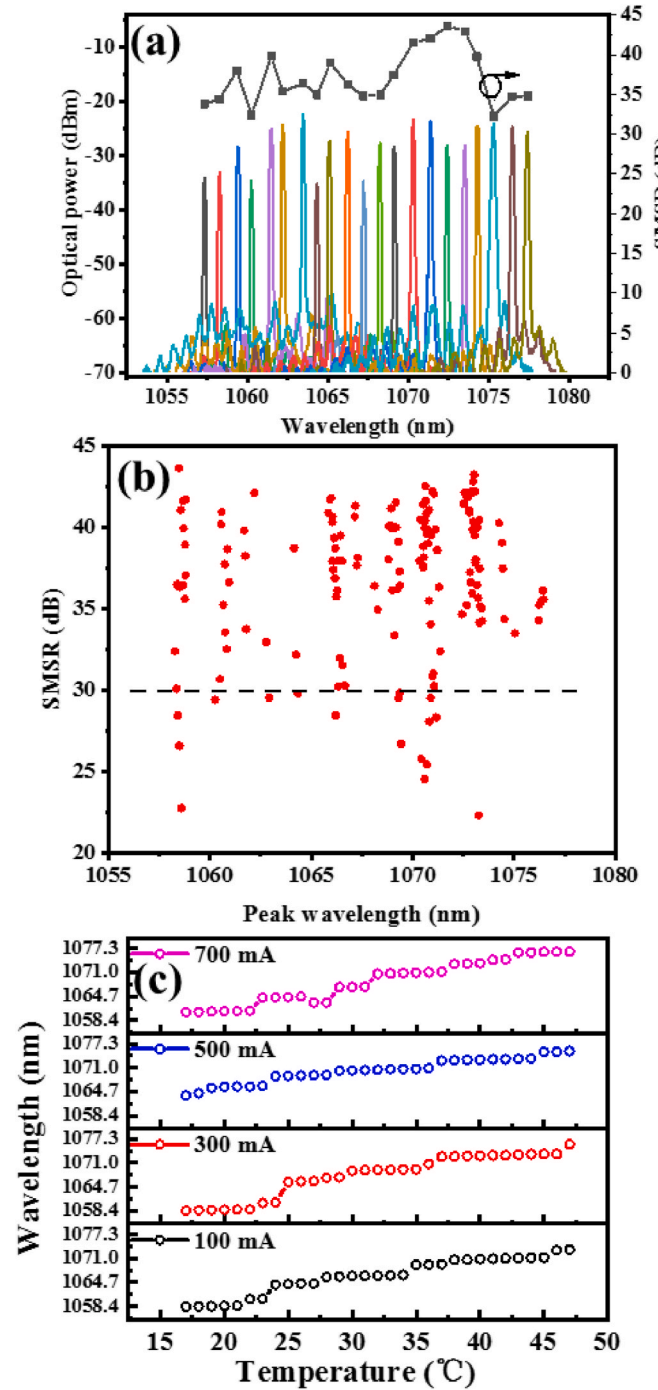


Fig. 5. (a) The measured spectrum of the device with tuning range of 20 nm. (b) SMSR values of different lasing wavelengths under varying injection current from 100 mA to 700 mA with a step of 100 mA and temperature from 17 °C to 47 °C with a step of 1 °C. Points with SMSR below 20 dB are not drawn. (c) Measured peak wavelengths change as the temperature under different currents.

where Γ is the optical limiting factor of the active region, g_{material} is the material gain, α_i is the internal loss, L is the efficient cavity length, R_f and R_{DBR} is the reflectivity of the front cavity surface and the grating section of the device, respectively. The Γ , α_i , L , and R_f can be considered as the constant term. The right-hand side of equation (1) can be called mode loss and is only relevant to the R_{DBR} . And the left-hand side of the equation is called mode gain. The calculated mode loss and mode gain of the device vary with temperature is shown in Fig. 6(a). At 17 °C, the

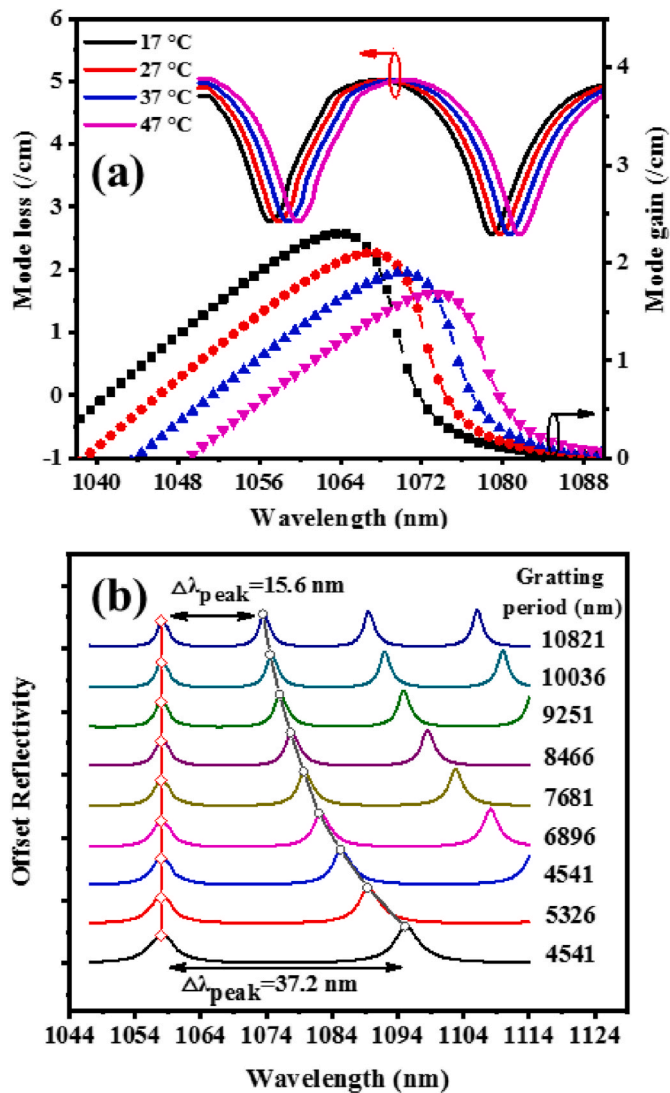


Fig. 6. (a) The calculated mode loss and mode gain of the device vary with temperature. (b) The calculated reflectivity curves and the interval of wavelengths between two adjacent peaks of reflectivity under different grating periods.

peak of the mode gain is close to the first valley of the mode loss, and the device emits the laser near the wavelength corresponding to the first valley of the mode loss. As the temperature increases from 17 °C to 47 °C, the mode loss spectrum is redshifted by ~ 3 nm [21], while the mode gain spectrum is redshifted by ~ 15 nm. At 47 °C, the peak of the mode gain is close to the next valley of the mode loss, and the device emits the laser near the longer wavelength corresponding to the second mode loss valley. Fig. 6(b) depicts the reflectivity and reflectivity peak spacing $\Delta\lambda_{\text{peak}}$ of the surface grating with a different grating period. The $\Delta\lambda_{\text{peak}}$ decreases with the increase of the grating period, and the downward trend is gradually gentle. When the grating period is small, the $\Delta\lambda_{\text{peak}}$ is larger than the FWHM of the gain spectrum of the general quantum well (~ 20 nm). As a result, the gain spectrum cannot be timely intersected with the two adjacent loss valleys through temperature induction, and the wide tuning cannot be realized. The P-I-V characteristic at different temperatures of the device is shown in Fig. 7. With the temperature increasing from 17 °C to 47 °C, the threshold current of this laser increasing from 70 mA to 100 mA and the maximum output power decrease from 105 mW to 90 mW.

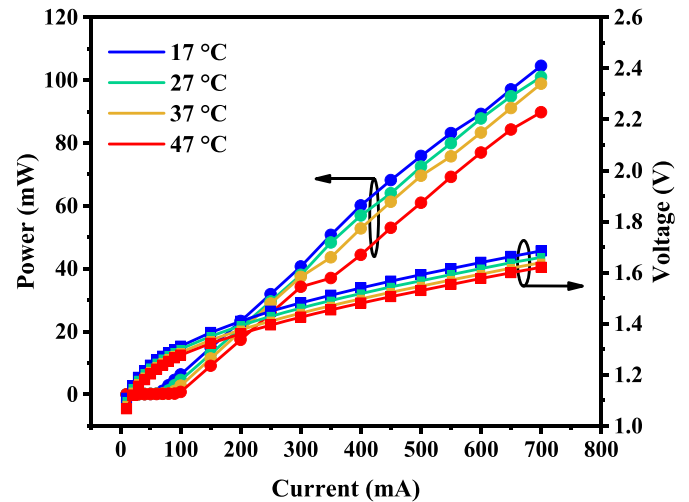


Fig. 7. The change of power and voltage with current at different temperatures.

4. Conclusion

In this paper, a wide-tuning slotted high-order surface grating laser is realized. By adjusting the current and temperature, a tuning range of 20 nm with SMSRs large than 30 dB is achieved. The maximum output power of the device is 112 mW. Preliminary analysis shows that this wide tuning range results from the temperature-induced gain spectrum shifting between two adjacent Bragg reflection peaks of the high-order surface grating.

Credit author statement

Yinli Zhou (First Author): Conceptualization, Methodology, Software, Investigation, Formal analysis, Writing – original draft; Jianwei Zhang (Corresponding Author): Conceptualization, Resources, Supervision, Writing – review & editing. Xing Zhang: Visualization, Investigation; Yongqiang Ning: Resources, Supervision, Funding acquisition; Yugang Zeng: Investigation, Software. Lijun Wang: Project administration.

Declaration of competing interest

The authors declare that they have no known competing financial interests or personal relationships that could have appeared to influence the work reported in this paper.

Acknowledgements

This work is supported by National Key Research and Development Program (2020YFC2200300); National Natural Science Foundation of China (NSFC) (Nos. 52172165, 61804151, 62090060, 61874117, 11774343, 61874119), Science and Technology Development Project of Jilin Province (20200401006GX).

References

- [1] M.C. Bustillos Barcaya, G.F. Rinalde, Embedded tunable laser control for WDM optical communications systems, *IEEE Latin Am. Trans.* 18 (2) (2020) 241–248.
- [2] Y.M. Su, Y. Bi, P.F. Wang, J. Sun, X.Y. Sun, S. Luo, J.Q. Pan, Y.J. Zhang, Emitting direction tunable slotted laser array for Lidar applications, *Opt Commun.* 462 (2020) 125277.
- [3] R. Sur, Y. Ding, R. Jackson, R. Hanson, Tunable laser-based detection of benzene using spectrally narrow absorption features, *Appl. Phys. B* 125 (2019) 195.
- [4] L.A. Coldren, G.A. Fish, Y. Akulova, J.S. Barton, L. Johansson, C.W. Coldren, Tunable semiconductor lasers: a tutorial, *J. Lightwave Technol.* 22 (1) (2004) 193–202.
- [5] S. Sakano, T. Tsuchiya, M. Suzuki, S. Kitajima, N. Chinone, Tunable DFB laser with a striped thin-film heater, *IEEE Photon. Technol. Lett.* 4 (4) (1992) 321–323.

- [6] L. Han, S. Liang, J. Xu, L. Qiao, H. Wang, L. Zhao, H. Zhu, W. Wang, DBR laser with over 20-nm wavelength tuning range, *IEEE Photon. Technol. Lett.* 28 (9) (2016) 943–946.
- [7] Y. Tohmori, Y. Yoshikuni, H. Ishii, Broad-range wavelength-tunable superstructure grating (SSG) DBR lasers, *IEEE J. Quant. Electron.* 29 (1993) 1817–1823.
- [8] J. Zhao, S. Hu, Y. Tang, H. Zhao, Y. Yu, Widely tunable semiconductor laser based on digital concatenated grating with multiple phase shifts, *IEEE Photonics J* 5 (5) (2013) 1502008.
- [9] A.J. Ward, D.J. Robbins, G. Busico, E. Barton, L. Ponnampalam, J.P. Duck, N. D. Whitbread, P.J. Williams, D.C.J. Reid, A.C. Carter, M.J. Wale, Widely tunable DS-DBR laser with monolithically integrated SOA: design and performance, *IEEE J. Sel. Top. Quant. Electron.* 11 (1) (2005) 149–156.
- [10] M. Tawfieq, H. Wenzel, P. Della Casa, O. Brox, A. Ginolas, P. Ressel, D. Feise, A. Knigge, M. Weyers, B. Sumpf, G. Tränkle, High power sampled-grating based MOPA system with 23.5 nm wavelength tuning around 970 nm, *Appl. Opt.* 57 (2018) 8680–8685.
- [11] S. Zhang, J. Meng, S. Guo, L. Wang, J.J. He, Simple and compact V-cavity semiconductor laser with 50×100 GHz wavelength tuning, *Opt Express* 21 (11) (2013) 13564–13571.
- [12] F. Dong, F. Du, P. Ma, X. Zhou, W. Zheng, 30-nm consecutive discrete tuning range semiconductor laser with 100-GHz channel spacing based on slotted structures fabricated by standard contact lithography, in: *Conference on Lasers and Electro-Optics, OSA Technical Digest (Optical Society of America, 2020 paper JTh2D.12.*
- [13] M. Nawrocka, Q. Lu, W.H. Guo, A. Abdullaev, F. Bello, J. O'Callaghan, T. Cathcart, J.F. Donegan, Widely tunable six-section semiconductor laser based on etched slots, *Opt Express* 22 (16) (2014) 18949–18957.
- [14] M. McDermott, R. McKenna, C. Murphy, D. Mickus, H.Z. Weng, S. Naimi, Q.Y. Lu, W.H. Guo, M. Wallace, N. Abadía, J.F. Donegan, 1.3 μm wavelength tunable single-mode laser arrays based on slots, *Opt Express* 29 (10) (2021) 15802–15812.
- [15] F. Dong, A. Liu, P. Ma, M. Wang, W. Zheng, 20-nm consecutive discrete tuning range semiconductor laser with 125-GHz channel spacing based on slotted surface grating fabricated by standard lithography, *Semicond. Sci. Technol.* 35 (2020), 045018.
- [16] A. Abdullaev, Q. Lu, W. Guo, M.J. Wallace, M. Nawrocka, F. Bello, A. Benson, J. O'Callaghan, J.F. Donegan, Improved performance of tunable single-mode laser array based on high-order slotted surface grating, *Opt Express* 23 (9) (2015) 12072–12078.
- [17] J.W. Zimmerman, R.K. Price, U. Reddy, N.L. Dias, J.J. Coleman, Narrow linewidth surface-etched DBR lasers: fundamental design aspects and applications, *IEEE J. Sel. Top. Quant. Electron.* 19 (4) (2013) 1503712.
- [18] W.H. Guo, Q. Lu, M. Nawrocka, A. Abdullaev, J. O'Callaghan, J.F. Donegan, Nine-channel wavelength tunable single mode laser array based on slots, *Opt Express* 21 (8) (2013) 10215–10221.
- [19] S. E, Y. Zhou, X. Zhang, J. Zhang, Y. Huang, Y. Zeng, J. Cui, Y. Liu, Y. Ning, L. Wang, High-order DBR semiconductor lasers: effect of grating parameters on grating performance, *Appl. Opt.* 59 (28) (2020) 8789–8792.
- [20] Q. Lu, W.H. Guo, D. Byrne, J.F. Donegan, Design of slotted single mode lasers suitable for photonic integration, *IEEE Photon. Technol. Lett.* 22 (11) (2010) 787–789.
- [21] F. Bello, M.J. Wallace, R. McKenna, G. Jain, Q.Y. Lu, W.H. Guo, J.F. Donegan, Athermal tuning for a two-section, all-active dbr laser with high-order grating, *IEEE Photonics J* 10 (2018) 1–11.
- [22] D. Byrne, J. Engelstaedter, W. Guo, Q. Lu, B. Corbett, B. Roycroft, J. O'Callaghan, F.H. Peters, Discretely tunable semiconductor lasers suitable for photonic integration, *IEEE J. Sel. Top. Quant. Electron.* 15 (3) (2009) 482–487.